
STATISTICAL ANALYSIS OF THERMAL CONDUCTIVITY EXPERIMENTALLY MEASURED IN WATER-BASED NANOFLUIDS

A PREPRINT

J. Tielke¹, M. Maas^{2,3}, M. Castillo¹, K. Rezwan^{2,3} and M. Avila^{*1,3}

¹University of Bremen, Center of Applied Space Technology and Microgravity (ZARM),
Am Fallturm 2, 28359 Bremen, Germany

²University of Bremen, Advanced Ceramics,

Am Biologischen Garten 2, 28359 Bremen, Germany

³MAPEX Center for Materials and Processes, University of Bremen,
28359 Bremen, Germany

January 7, 2022

ABSTRACT

Nanofluids are suspensions of nanoparticles in a base heat-transfer liquid. They have been widely investigated to boost heat transfer since they were proposed in the 1990's. We present a statistical correlation analysis of experimentally measured thermal conductivity of water-based nanofluids available in the literature. The influences of particle concentration, particle size, temperature and surfactants are investigated. For specific particle materials (alumina, titania, copper oxide, copper, silica and silicon carbide), separate analyses are performed. The conductivity increases with the concentration in qualitative agreement with Maxwell's theory of homogeneous media. The conductivity also increases with the temperature (in addition to the improvement due to the increased conductivity of water). Surprisingly, only silica nanofluids exhibit a statistically significant effect of the particle size, whereby smaller particles lead to faster heat transfer. Overall, the large scatter in the experimental data prevents a compelling, unambiguous assessment of these effects. Taken together, the results of our analysis suggest that more comprehensive experimental characterizations of nanofluids are necessary to estimate their practical potential.

1 Introduction

The efficient removal of heat with circulating fluids is pivotal to applications in mechatronics, mechanical, aerospace and chemical engineering. The main limiting material property in heat transfer is the thermal conductivity (k) of the fluid, followed by the viscosity. Conventional liquids used for heat transfer, such as water or ethylene glycol, are inexpensive but exhibit low k -values. In an influential paper published in 1995, Stephen U.S. Choi and Jeffrey A. Eastman [1] proposed that ‘*an innovative class of heat transfer fluids can be engineered by suspending metallic nanoparticles in conventional heat transfer fluids. The resulting nanofluids are expected to exhibit high thermal conductivities*’. Their experimental measurements with ethylene glycol exhibited an increase in thermal conductivity up to 20% at a volume fraction of 4% through the addition of copper oxide particles ($d \approx 20$ nm) and spurred many theoretical and experimental investigations [2]. Several models were proposed to explain what was historically termed as anomalous heat transfer, meaning that the effective material properties of the suspension (e.g. effective viscosity and thermal conductivity of the nanofluid) could not solely account for the enhanced heat transfer [3, 4]. In an influential paper, Buongiorno [5] considered many possible physical mechanisms behind convective heat transfer enhancement in nanofluids and assessed their plausibility and relative importance. He argued that Brownian motion and thermophoresis (i.e. the motion of particles along gradients of temperature) were the two only plausible mechanisms for heat transfer enhancement. Keblinski *et al.* [6] critically analysed some experimental data sets and concluded that effective medium theories are capable of explaining the data.

*correspondence to: marc.avila@zarm.uni-bremen.de

In 2009, Buongiorno *et al.* [7] performed an experimental benchmark study to determine the influence of the measurement technique on the experimental thermal conductivity of nanofluids. This study showed that the data scattered in a range of at least $\pm 5\%$ about the median, which implied that a total enhancement of a few percent cannot be detected. Subsequently, Khanafer *et al.* [8] developed correlations for thermal conductivity and viscosity based on experimental data. There have been no additional benchmark studies or statistical analysis since their study. Characterization efforts have mainly focused on the analysis of the nanoparticle sizes and particle concentrations [9–13].

Recently, the state of the art in this field was reviewed by Buschmann *et al.* [14], who analyzed several experiments on convective heat transfer with nanofluids. Their analysis supported the conclusion of Buongiorno [5] that there are no anomalies in the convective or conductive heat transfer of nanofluids. Buschmann *et al.* [14] argued that nanofluids can be treated as homogeneous fluids by considering their effective properties. Hence, their heat transfer can be correctly predicted by well-established correlations for pure fluids, provided that the effective thermal conductivity and the effective viscosity of the nanofluid are known. Finally, Buschmann *et al.* [14] pointed out that there is currently a lack of knowledge of how and why nanoparticles change the thermal conductivity of a fluid.

The observation that thermophysical properties are modified by additions of particles to a fluid dates back to the theoretical work of Maxwell in 1881 [15]. According to his Effective Medium Theory, the effective thermal conductivity of a nanofluid k_{eff} depends on the thermal conductivities of the nanoparticles k_p , thermal conductivity of the base fluid k_f , and particle fraction φ ,

$$\frac{k_{\text{eff}}}{k_f} = 1 + \frac{3\varphi(k_p - k_f)}{3k_f + (1 - \varphi)(k_p - k_f)}. \quad (1)$$

Eapen *et al.* [16] argued that there may be different dispersion states in nanofluids that influence thermal conductivity, which are not considered in Maxwell's theory. For example, particles can form percolating structures at moderately low concentrations [16, 17]. Through the use of a theory developed by Hashin and Shtrikman [18], Eapen *et al.* [16] derived the following HS-bounds for the effective thermal conductivity of nanofluids

$$k_f \left[1 + \frac{3\varphi(k_p - k_f)}{3k_f + (1 - \varphi)(k_p - k_f)} \right] \leq k_{\text{eff}} \leq k_p \left[1 - \frac{3(1 - \varphi)(k_p - k_f)}{3k_p - \varphi(k_p - k_f)} \right] \quad (2)$$

The lower HS-bound represents the well-dispersed state, where the particles are the disperse phase and the base fluid is the continuous phase, which was already described by Maxwell, see eq. (1). Hence, in the well-dispersed state, heat is mainly transferred through the fluid. The upper HS-bound represents a state in which heat is mainly transferred between particles [16, 18, 19]. Specifically, at high concentrations ($\varphi \approx 1$), the base fluid becomes the dispersed phase and particles the continuous phase. Even if this limit is not realistic for e.g. spherical particles (due to close-packing), it is still useful in describing particle configurations (chains, percolation networks), which can arise even at low concentrations and result in strongly enhanced heat transfer [20].

Maxwell's and Hashin and Shtrikman's theories of suspensions do not account for the particle size, whereas the distinct feature of nanofluids is that the particles are less than 100 nm in one dimension. Vadasz *et al.* [21] considered heat conduction in nanofluids and reviewed the transient-hot-wire method. He showed that by accounting for the dependence of the heat transfer coefficient on the particle size (through the particle's specific area S), the experimental data became consistent with classical theories of suspensions. However, he stated that his analysis was inconclusive and that more experimental data were required. Further experimental studies [11, 22–25] showed that thermal conductivity increases linearly with increasing temperature and suggested an effect from the particle size.

Bouguerra *et al.* [20] recently showed that the effective thermal conductivity and the effective viscosity of water-based alumina nanofluids strongly depend on pH. They were able to distinguish between different dispersion states that included well-dispersed particles, the formation of percolation networks, and fully agglomerated particles, through measurements with volume concentrations between 0.2% and 2% at different pH levels. Variations of the pH modify the suspension stability through repulsive forces of electrostatic origin. An alternative to this is the use of surfactants. Depending on the choice and concentration of the surfactant, the thermal conductivity of the nanofluid may be increased or decreased [12, 26–30], and to date there is no general, coherent picture as to what the effect of surfactants on the nanofluid is.

In this paper, we present a statistical correlation analysis of thermal conductivity measurements of water-based nanofluids available in the scientific literature. The aim of our analysis is to assess nanofluids for potential applications and to identify suitable nanomaterials for heat transfer. To this avail, we analyze whether the influences of particle concentration, size, temperature and surfactants on the thermal conductivity of nanofluids are statistically significant, and we quantify their relative importance.

2 Material and Methods

We compiled a database with $N = 1656$ data points (experimental measurements of the thermal conductivity) from 73 publications concerned with water-based nanofluids. The data points were taken from publications in which temperature, volume concentration, and particle size were fully specified. The database is given in the supplementary materials and contains data for 17 different nanoparticle materials. In the first part of our analysis, all data points were considered. Subsequently, six individual materials were analyzed for which there are at least 4 different publications available comprising $N \geq 50$ data points altogether. This was done to avoid spurious results due to small samples. The six individual materials are:

- Alumina (Al_2O_3 , $N = 470$): [2, 9, 12, 13, 20, 22–24, 31–57]
- Titania (TiO_2 , $N = 188$) [44, 50, 57–63]
- Copper oxide (CuO , $N = 106$) [12, 22, 24, 44, 52, 56, 64]
- Copper (Cu , $N = 94$) [26, 27, 56, 65, 66]
- Silica (SiO_2 , $N = 86$) [13, 32, 67–72]
- Silicon carbide (SiC , $N = 53$) [73–77]

Descriptive statistics for these data sets are shown in table 1 of the supplementary materials. We note that for the analysis of copper nanofluids we excluded the study of Liu [65]. This study features results which are very different from those of all other works for the same material. The decision to exclude them is further justified later. Here it suffices to say that as a result of excluding this, the regression significantly improves. For completeness, a comparison to the regressions with all data points (without exclusion) can be found in the supplementary materials.

For the materials below there are less than 4 publications and/or less than 50 data points. Thus we did not analyze them individually, because the analysis would have little statistical significance:

- Iron(III)oxide (Fe_2O_3 , $N = 86$) [78, 79]
- Iron(II,III)oxide (Fe_3O_4 , $N = 98$) [80–82]
- Zinc oxide (ZnO , $N = 3$) [50]
- Graphene (G , $N = 145$) [28, 83, 84]
- Graphene oxide (GO , $N = 20$) [85]
- Carbon-Nanotubes (CNT, $N = 188$) [28, 29]
- Nanodiamond (ND, $N = 38$) [86, 87]
- Silver (Ag , $N = 34$) [68, 70, 88, 89]
- Iron (Fe , $N = 15$) [90]
- Aluminum (Al , $N = 20$) [56]
- Gold (Au , $N = 4$) [91, 92]

We caution that the published data for metals have to be interpreted critically because metallic particles easily oxidize in water [93, 94].

2.1 Linear statistical model

We employed a linear model to statistically quantify the effect of the volume concentration φ , the temperature T and the particle size (through the specific surface S) on the normalized thermal conductivity

$$k^*(\varphi, T, S) = \frac{k_{\text{eff}}(\varphi, T, S)}{k_f(T)}, \quad (3)$$

where $k_f(T)$ is the thermal conductivity of the base fluid (pure water) as a function of the temperature. Changes in the thermal conductivity of the base fluid k_f due to the addition of surfactants or changes in the pH were taken account of, if the data were specified in the respective studies. Nevertheless, most of the data are given normalized or are normalized on pure water.

Our linear statistical regression model reads

$$k^*(\varphi, T, S) = C_0 + C_\varphi \varphi + C_T T^* + C_S S^*, \quad (4)$$

where the coefficients C_i (with $i = \{0, \varphi, T, S\}$) were determined from linear regressions of the data sets. These coefficients are dimensionless, due to the definitions of $T^* = (T - T_{\text{ref}})/T_{\text{ref}}$ and $S^* = (S - S_0)/S_{\text{ref}}$. We chose $T_{\text{ref}} = 293$ K because most measurements found in the literature were taken at room temperature. For large particles (with specific surface $S \approx 0$), we do not expect an increase in thermal conductivity beyond Maxwell's theory, therefore we chose $S_0 = 0$ as reference. Finally, we chose $S_{\text{ref}} = 6/d_{\text{ref}}$ with $d_{\text{ref}} = 1$ nm for simplicity (with these choices the last term simplifies to $S^* = S/S_{\text{ref}} = d_{\text{ref}}/d$).

2.2 Physical interpretation of the linear statistical model

Starting with Maxwell's equation (1) and linearizing about zero concentration ($\varphi=0$), one obtains a linear prediction of the normalized effective thermal conductivity for small concentrations

$$k^*(\varphi) = 1 + C_{\varphi, \text{Maxwell}} \varphi, \quad (5)$$

where

$$C_{\varphi, \text{Maxwell}} = 3 \frac{(k_p - k_f)}{(k_p + 2k_f)}. \quad (6)$$

The coefficient $C_{\varphi, \text{Maxwell}}$ increases monotonously as the thermal conductivity of the particles k_p increases. In particular, in the low conductivity limit ($k_p \ll k_f$), $C_{\varphi, \text{Maxwell}} = -1.5$, whereas in the opposite limit ($k_p \gg k_f$), $C_{\varphi, \text{Maxwell}} = 3$. Hence in the framework of the linear Maxwell's equation (5), $C_{\varphi, \text{Maxwell}} \in [-1.5, 3]$. This theoretical prediction can be compared with the coefficients obtained from the linear regression of (4) to the compiled data sets, whereby regression values with $C_{\varphi} > 3$ indicate higher performance than admissible in Maxwell's theory. For example, in the aforementioned experiments of Lee *et al.* [2], the heat transfer rates increased up to 20% at a volume fraction of 4% ($\varphi = 0.04$). This would imply $C_{\varphi} = 5$, which cannot be explained with Maxwell's theory. Furthermore, if there are no particles ($\varphi = 0$), the thermal conductivity must remain unchanged and it would be expected that the linear correlation analysis yielded values of $C_0 \approx 1$. The deviation of C_0 from unity serves as a proxy for the level of quality of the linear model and/or for the scatter of the data.

2.3 Data processing and statistical methods

Analyses were performed with IBM SPSS Statistics Version 25 using regressions with the normalized thermal conductivity (k^*) as a dependent variable and φ , T^* and S^* as independent variables. All variables were entered in a single step and confidence intervals were calculated to 95%. We evaluated the corrected correlation coefficient R^2 , the coefficients ($C_0, C_{\varphi}, C_T, C_S$), the standard deviations of the coefficients and the standardized regression coefficients ($\beta_{\varphi}, \beta_T, \beta_S$). The values of ($\beta_{\varphi}, \beta_T, \beta_S$) were calculated by subtracting the mean from the variable and dividing by its standard deviation. The larger the standardized regression coefficient of a parameter, the higher the influence of that parameter on k^* . Our analysis demonstrated that when $|\beta_i| < 0.1$ the influence of parameter i was insignificant.

Additional analyses were also carried out with subsets of the data or variations of the model, which allowed an assessment of the robustness of the data and model. For example, to verify the use of the linear regression in terms of the concentration, we restricted the data to $\varphi \leq 0.02$. The influence of surfactants was tested by performing separate regressions for the data without surfactants. Furthermore, we fitted nonlinear regressions with quadratic and cubic terms on the concentration and also with $C_0 = 1$ fixed. Detailed results for all the linear and nonlinear regressions can be found in the supplementary materials.

3 Results

The result of using a linear regression to fit all data points of our database with model eq. (4) is shown in the first row of table 1. In figure 1 the model prediction (vertical axis) is plotted against the experimentally measured normalized thermal conductivity (horizontal axis). Data points lying along the black line exhibit perfect agreement with our linear model, eq. (4), whereas the discrepancy is larger the further the data points are from the line. The shaded region depicts a $\pm 10\%$ interval about the model prediction. The correlation coefficient is $R^2 = 0.29$ and $C_0 = 1.031$. The most significant parameter is the concentration, with $C_{\varphi} = 1.81$ ($\beta_{\varphi} = 0.39$), which is well within the bounds from the linearized Maxwell equation, $C_{\varphi, \text{Maxwell}} \in [-1.5, 3]$. The thermal conductivity also increases with increasing temperature and specific surface, with $C_T = 0.51$ ($\beta_T = 0.27$) and $C_S = 0.092$ ($\beta_S = 0.34$), respectively. These results allow a first estimation of the performance of water-based nanofluids. For example, if $d = 30$ nm at a 4% concentration and $T = 303$ K is substituted into eq. (4)

$$k^* = C_0 + C_{\varphi} \varphi + C_T T^* + C_S S^* = 1.031 + 0.072 + 0.017 + 0.003 = 1.124,$$

Table 1: Results of the linear regressions fitted to the entire database and for each individual material, with the number of data points (N), corrected correlation coefficient (R^2), model coefficients (C_φ, C_T, C_S), and their corresponding standardized correlation coefficients ($\beta_\varphi, \beta_T, \beta_S$)

Material	N	R^2	C_0	C_φ	β_φ	C_T	β_T	C_S	β_S
General	1656	0.29	1.031	1.81	0.39	0.51	0.27	0.092	0.34
Alumina	470	0.53	1.025	1.75	0.72	0.31	0.21	0.16	0.12
Titania	188	0.75	1.018	1.69	0.58	0.63	0.51	-0.19	-0.097
Copper oxide	106	0.23	1.051	1.45	0.54	0.27	0.20	-0.47	-0.057
Copper	94	0.43	1.059	7.46	0.72	-0.24	-0.086	0.48	0.073
Silica	86	0.27	0.994	0.61	0.35	0.10	0.31	0.42	0.47
Silicon carbide	53	0.68	1.082	2.97	0.70	-0.018	-0.017	-1.25	-0.25

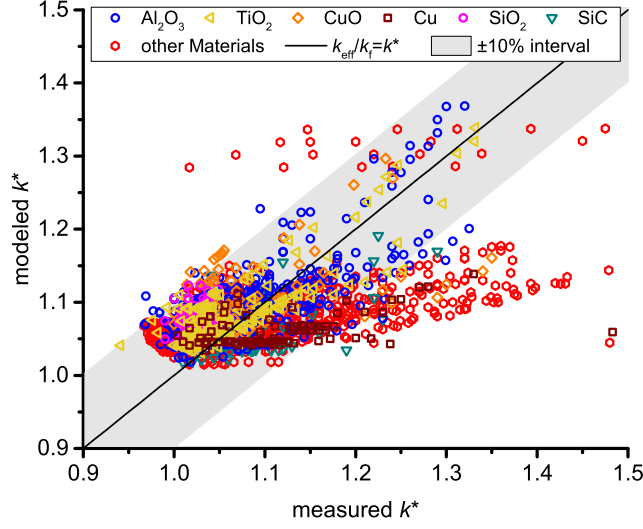


Figure 1: Experimentally measured versus modeled normalized thermal conductivity (k^*) for water-based nanofluids. The ideal values of k^* and a $\pm 10\%$ interval are displayed as a solid line and a grey area, respectively. Colors are used to distinguish single materials (analysed separately) from other materials (see the legend). The model is $k^* = 1.031 + 1.81 \varphi + 0.51 T^* + 0.092 S^*$ ($R^2 = 0.29$, $N = 1656$).

a 12.4% increase in thermal conductivity is obtained (when compared to pure water at $T = 303$ K). Noteworthy, the contribution directly from the particle size (last term) is negligible.

The linear regressions to the data sets for single materials are shown in figure 2. Clearly, the scatter in the data and the goodness of the fit depend strongly on the material, which is quantified by the respective R^2 (given in the second column of table 1). Overall, the values of β_φ given in the fourth column of table 1 confirm that increasing the particle concentration leads to a statistically significant enhancement of the thermal conductivity for all materials analyzed. In addition, there is also a significant influence of the temperature and/or surface for specific materials (see the sixth and eight columns of table 1). In what follows, we discuss the influence of each of these three factors separately.

3.1 Effect of particle concentration

The computed values of C_φ are shown in figure 3a as a function of the thermal conductivity of the particle material. The corresponding 95% confidence intervals indicate that silicon carbide nanofluids are in excellent agreement with Maxwell's prediction (eq. (5) and lower solid line in the figure), whereas silica, alumina, titania and copper oxide nanofluids are below it. Only copper nanofluids appear to exceed Maxwell's prediction. Overall, the discrepancy with Maxwell's prediction is not large in view of the large scatter in the data sets. By linearizing the upper HS-bound of eq. (2), we obtained an upper bound for C_φ (upper solid line in figure 3a). This upper bound embraces all possible dispersion states and is satisfied also by copper.

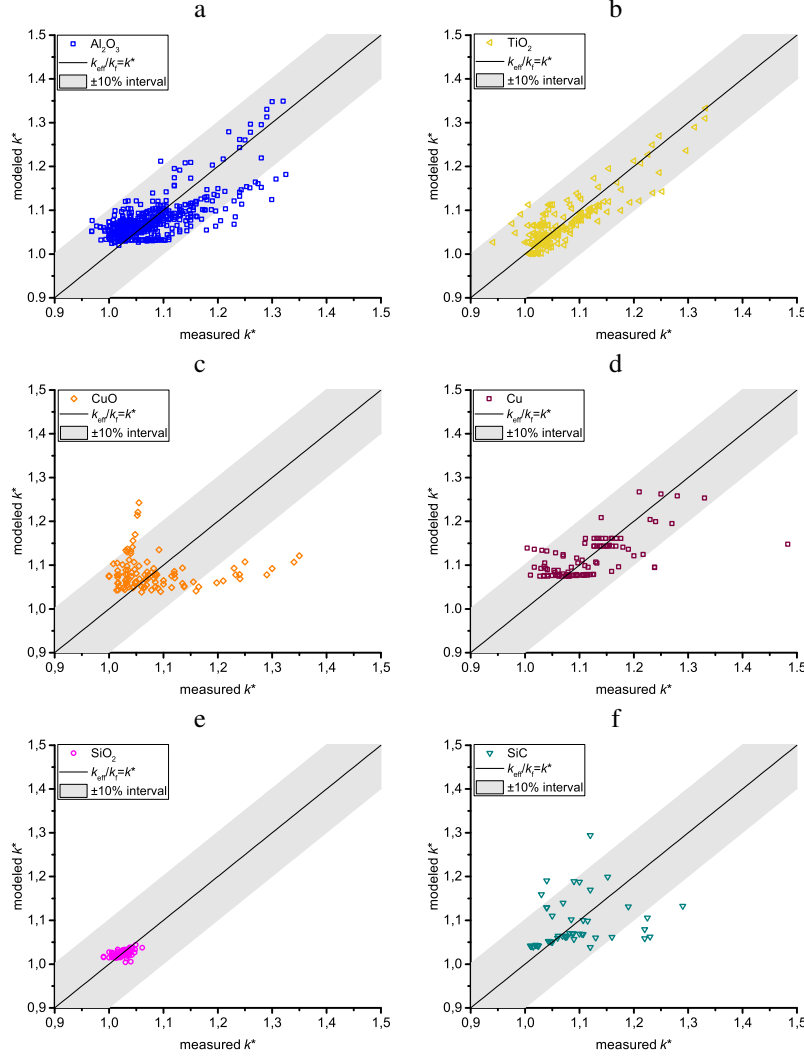


Figure 2: Experimentally measured versus modeled normalized thermal conductivity (k^*). The ideal values of k^* and a $\pm 10\%$ interval are displayed as a solid line and a grey area, respectively. (a) Alumina with $N = 470$ and $k^* = 1.025 + 1.75 \varphi + 0.31 T^* + 0.16 S^*$ ($R^2 = 0.53$). (b) Titania with $N = 188$ and $k^* = 1.018 + 1.69 \varphi + 0.63 T^* - 0.19 S^*$ ($R^2 = 0.75$). (c) Copper oxide with $N = 106$ and $k^* = 1.051 + 1.45 \varphi + 0.27 T^* 0.48 S^*$ ($R^2 = 0.23$). (d) Copper with $N = 94$ and $k^* = 1.059 + 7.46 \varphi + -0.24 T^* 0.48 S^*$ ($R^2 = 0.43$). (e) Silica with $N = 86$ and $k^* = 0.42 + 0.61 \varphi + 0.10 T^* + 0.42 S^*$ ($R^2 = 0.27$). (f) Silicon carbide with $N = 53$ and $k^* = 1.082 + 2.97 \varphi + -0.018 T^* - 1.25 S^*$ ($R^2 = 0.68$).

3.2 Effect of nanofluid temperature

The computed values of C_T for single materials are shown in figure 3b. Increasing the temperature in titania nanofluids enhances the thermal conductivity significantly and strongly. For alumina and copper oxide nanofluids the increase in thermal conductivity is less pronounced and also less significant. For silica the effect is significant, but the performance increase is even weaker. Finally, there is no significant influence of temperature on the thermal conductivity for copper and silicon carbide nanofluids, which is due to a lack of experimental measurements for a sufficiently large range of temperatures (see table 1, figs. 5 and 7 in the supplementary material).

3.3 Effect of the particle size

The computed values of C_S are shown in figure 3c. A strong effect of the particle size is found only in silica nanofluids ($C_S = 0.42$, $\beta_S = 0.47$). For alumina nanofluids the particle size has a mildly significant and weak effect. In both cases, reducing the particle size appears to enhance the thermal conductivity. By contrast, for silicon carbide nanofluids the computed coefficient is negative ($C_S = -1.25$), suggesting that increasing the particle size leads to higher thermal conductivity. However, the large scatter in the data for this material (see the corresponding confidence intervals in figure 3c) does not allow a conclusive statement. For copper oxide and copper nanofluids the effect is statistically insignificant, which may be attributed to the absence of variation in particle size in the experimental measurements available (see table 1, fig. 2 in the supplementary material).

The case of titania is more complicated to interpret. Here the experimental measurements span a wide range of particle sizes, yet the particle-size effect is insignificant if all data are used. If only the measurements without surfactant are considered in the statistical analysis, the particle size appears to have a very strong and significant influence, with $C_S = 1.931$ and $\beta_S = 0.367$. The descriptive statistics and boxplot diagram in the supplementary material (see figs. 2 and 4 therein) show an irregular distribution of the measured particle sizes, with most measurements for $d = 21$ nm and a few for 100 nm. This may result in the significant regression coefficients.

3.4 Effect of surfactants

Out of $N = 1656$ data points, 1038 data points (62%) were obtained in suspensions without surfactants, whereas 618 (38%) data points were obtained with surfactants. Half of these data points (309) were from surfactant concentrations of less than 1.67wt%, the rest with concentrations higher than 10wt% (225 data points) or provided no information about the concentration (84 data points). Descriptive statistics and corresponding boxplots can be found in section 2.2 in the supplementary materials. Depending on the type of the surfactant and concentration, the thermal conductivity of both, the base fluid and the nanofluid, may increase or decrease [12, 26–29]. Because of the heterogeneity of the measurements with surfactants (in type and concentration), it would be meaningful to analyze data with similar surfactant configurations together. However, this would lead to small data subsets and would prevent statistically significant analyses. Hence, in this work we statistically investigated the effect of surfactants by performing regressions of the data points obtained without surfactants (separately for each material), and then comparing the results to those presented in the previous sections (with and without surfactants).

The data for copper were all obtained with surfactants except for the study of Liu *et al.* [65]; this is the reason why their work was excluded from the analysis for copper. For SiO_2 and SiC nanofluids no surfactants were used. Hence the effect of surfactants cannot be investigated for these materials, as no comparisons (with/without surfactants) are possible. Still, we stress that the results for copper reveal a C_φ beyond Maxwell's theory in contrast to the other materials and insignificant C_T and C_S coefficients with large error-bars.

Comparisons were possible for Al_2O_3 and CuO , with (405/470) and (94/106) data points obtained without surfactants, respectively. The changes in the regressions of alumina and copper oxide without surfactants lie within the 95% intervals of the regression for the whole data sets. Major changes occurred in the case of TiO_2 . Out of $N = 188$ data points, 83 were obtained without surfactants. The concentration coefficient C_φ increases and nearly approaches Maxwell's prediction. The coefficients C_T and C_S increase beyond the 95% interval of the whole data set, whereas C_0 decreases.

Overall it can be concluded that while surfactants are expected to change the stability and the thermal conductivity of nanofluids, no conclusive statements can be made with the data available in the literature.

4 Discussion

Buongiorno *et al.* [7] pointed out already one decade ago that nanofluid data in the literature exhibit large scatter ($\pm 5\%$ about the median). A first critical statistical analysis of the scatter in the experimental data was done by Khanafer *et*

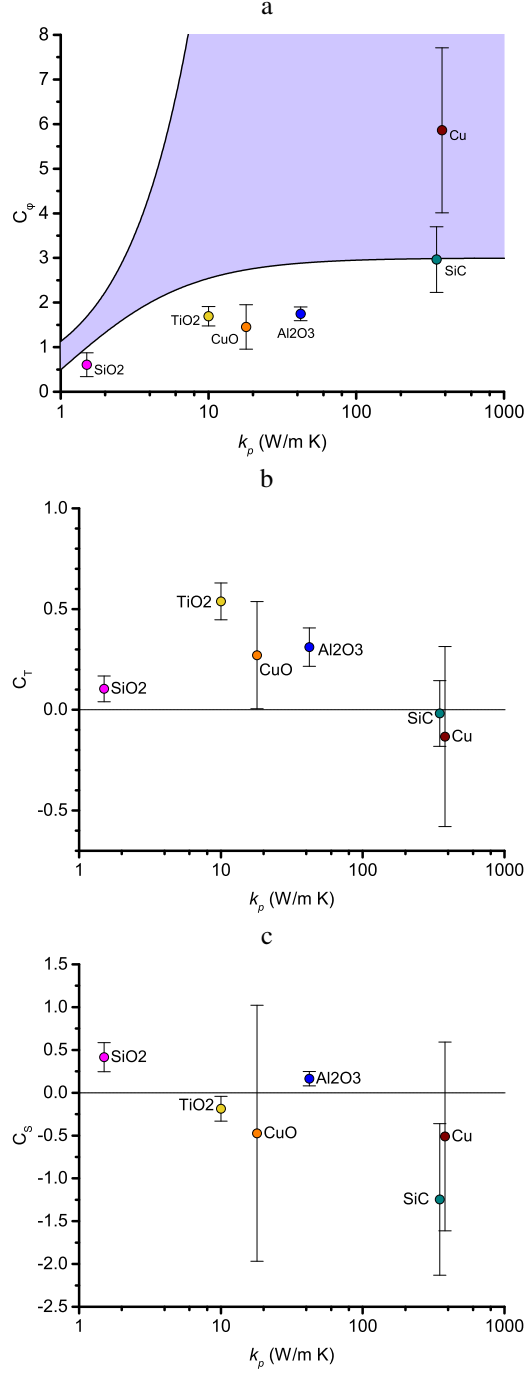


Figure 3: The colored symbols show the values of the model coefficient C_i (with corresponding 95% confidence-interval, shown as error-bars) as a function of the thermal conductivity k_p of each material. (a) Concentration coefficients C_ϕ . The linearized HS-bounds are displayed as solid black line. The lower bound is given by the linearized Maxwell equation (5), whereas the upper HS-bound was calculated by linearizing the right-hand-side of eq. (2) (with $\varphi k_p/k_f = 0$). (b) Temperature coefficients C_T . (c) Surface coefficients C_S .

al. [8]. Our statistical analysis extends and updates their analyses and confirms that the scatter in the different data sets is very large, as illustrated by the regression coefficients $R^2 \in [0.23, 0.75]$. In line with Buongiorno *et al.* [7], we attribute the large scatter in the data to two factors. First, the experimental determination of thermophysical properties (e.g. thermal conductivity) of fluids is known to be susceptible of errors (even for pure fluids). Chirico *et al.* [95] reviewed thermophysical data from five major journals and found errors in nearly one third of all publications. The most common problems were data with omitted uncertainties and the use of volume-based units [95]. Furthermore, in many publications the particle parameters (e.g. the size) were directly taken from the manufacturers, which is another source of error. Second, the characterizations of the nanofluids performed in the literature are often insufficient and additional variables need to be taken into account. Nieto de Castro *et al.* [96] considered the different factors influencing the thermal conductivity of nanofluids and emphasized the need for accurate, comparable measurements including stability characterizations (see [97, 98] also).

4.1 Dispersion state

The stability of nanofluids depends on their preparation, i.e. on the use of surfactants and/or the pH value of the fluid. For example, the colloidal stabilization of titania, alumina and other oxidic particles highly depends on pH [20], whereas hydrophobic particles (e.g. silicon carbide) agglomerate without the addition of dispersing agents [6, 99, 100]. Hence the surfactant itself and the concentration must be selected very carefully to maximize the thermal conductivity. Due to the heterogeneity in surfactant type and concentration (and particle material and size) used across studies, it is difficult to compare data and draw general conclusions from them. Hence, despite the widespread use of surfactants, the results are ambiguous at best. Many studies suggest improved thermal conductivity, whereas others suggest the opposite [12, 26–29]. The copper nanofluids in the literature were synthesized with the use of surfactants. In most studies, the concentration of surfactants was above the critical micelle concentration, possibly generating networks of micelles in the nanofluid. Hence the high value of C_φ obtained for copper may arise from a dispersion state different than well-dispersed particles. We note however that micellar aggregates, worm-like micelles and network structures increase the viscosity of the nanofluid [30, 101]. Thus, the use of high surfactant concentrations may lead to high thermal conductivities, but may be rather unfavorable for the application of nanofluids.

Our analysis employs a linear regression to assess the importance of concentration, temperature and specific surface. This precludes an investigation of combined effects, whereas surface (particle-size) effects may depend on the concentration. Unfortunately, the quality and quantity of the published data do not currently allow for a statistically significant analysis of such combined effects via the inclusion of nonlinear terms (e.g. of the form $C_{\varphi,S} \varphi S^*$). We note however that we did not find any significant cross-correlations between variables. The aging and stability of the nanofluid, which change the dispersion state, could not be included in our statistical analysis, because these factors are seldom described in sufficient detail in published data [7, 102, 103]. For the same reason, we could not analyze the dependence of the effective viscosity on concentration, temperature and size of the nanoparticles.

The viscosity is crucial in heat transfer applications and complex structures, such as particle clusters or percolation networks, dramatically increase the viscosity of suspensions. Bouguerra *et al.* [20] have shown that for alumina nanofluids the well-dispersed regime (when available), is the preferred one for heat transfer applications. Studies employing molecular dynamics simulations have also shown that clustering influences the thermal conductivity of nanofluids [104–106], and increases their viscosity [104, 105]. Tahmooressi *et al.* [106] showed for nanoparticles at high concentrations ($\varphi = 0.1$) that the agglomeration of nanoparticles into small clusters may be more efficient towards high thermal conductivities than well-dispersed particles or percolating networks. This is in line with the experimental observations of Bouguerra *et al.* [20] measuring higher thermal conductivities for percolation than for dispersed particles. Clearly, simultaneous measurements of thermal conductivity and viscosity, and direct measurements of the state of dispersion of the nanofluid would be very useful. Here the determination of the diffusion coefficient and the size of the hydration layer would help [19, 107, 108].

4.2 Regressions with $C_0 = 1$

We also fitted all data sets discussed above, but imposing $C_0 = 1$ in eq. (4). The results are shown in table 6a–g and figs. 5–7 in the supplementary materials. For silica nanofluids the results do not change much when $C_0 = 1$ is imposed. For all other particle materials, imposing $C_0 = 1$ leads to an increase in the values of C_φ , C_T and C_S . This is because for all these materials $C_0 > 1$ in the linear regressions. In fact, the larger the value of C_0 in the linear regression, the larger the increase of the other coefficients when $C_0 = 1$ is set. For silicon carbide, copper oxide and copper nanofluids, the value of C_S even changes from negative to positive. Hence nothing can be said about particle size for these nanofluids. In both linear and nonlinear analyses the 95% confidence intervals for the surface coefficient C_S reflect the large scatter in the data regarding particle size effects. Overall, it can be concluded that setting $C_0 = 1$

does not qualitatively change the results of our analysis, but rather fortifies our findings and our assessment of the data quality.

4.3 Analysis for small concentrations $\varphi \leq 0.02$

We analysed the data for concentrations below 2% separately to assess the validity of the linear assumption for the concentration in our statistical regression model. We found statistically identical results for silica, silicon carbide and copper. For copper oxide, titania and alumina (see section 2.1 and figure 3 in the supplementary materials) the (relative) performance is better at low concentrations. For alumina, there is then perfect agreement with Maxwell, whereas titania and copper oxide are above the Maxwell curve, but with confidence intervals nearly touching it. It can be concluded that higher concentrations decrease the (relative) performance, possibly due to unfavourable agglomeration effects (see e.g. Bouguerra *et al.* [20]).

5 Conclusions and outlook

Our statistical analysis shows that the experimentally measured thermal conductivity of water-based nanofluids increases approximately linearly with the particle concentration. Within statistical uncertainty, this increase can be accounted for by Maxwell’s Effective Medium Theory for all materials. A possible exception may be copper nanofluids, although more experiments are necessary to assess their performance and the role of surfactants. A linear increase of the conductivity with the temperature was observed for all materials in which measurements covering sufficiently large temperature ranges are available. Finally, only silica nanofluids exhibit statistically significant, strong particle-size effects, which makes this scarcely investigated material interesting for fundamental investigations. In particular, in silica nanofluids, reducing the particle size (at constant concentration) leads to higher conductivity. Their performance is however low (compared to other nanofluids) because of their low value of C_φ .

In view of the detrimental effect of the increased viscosity and of stability issues, we suggest that the potential of nanofluids in engineering practice is limited. The main advantage of nanofluids, when compared to suspensions of larger particles, is their reduced sedimentation speed. We conclude that the large scatter found in the experimental measurements makes it difficult to test and compare theories for the effective thermal conductivity of water-based nanofluids. More comprehensive and precise characterizations, including the analysis of the dispersion state and of the stability on nanofluids (e.g. depending on the surfactant), are needed to quantify the sources of the data scatter. We believe that an improvement of the state of the art can only be achieved by ensuring the reproducibility of results with a priori identical conditions in different research groups. Silica nanoparticles are usually homogeneous in their size, are easy to handle and are sufficiently stable in dispersion. Hence, silica nanofluids are good candidates to precisely quantify the effects of particle size and dispersion stability on nanofluids. Copper nanofluids exhibit high thermal conductivities, but in order to compare their performance to other materials, it would be necessary to stabilize them with small concentrations of surfactant (below the critical micelle concentration). Unfortunately, this is challenging because metal nanoparticles rapidly oxidize and agglomerate without surfactants [109].

Finally, we suggest that more sophisticated statistical analyses [110, 111] could be employed to shed light on the source of the variability in the measured thermal conductivity of nanofluids. We will investigate possible factors in future work.

6 Competing Interests

The authors declare no competing interests.

7 Funding

his research did not receive any specific grant from funding agencies in the public, commercial, or not-for-profit sectors.

8 Acknowledgements

We thank Dr. Scharpenberg (Faculty Mathematics/Computer Science, University of Bremen) for critically reading an earlier version of the manuscript and providing helpful comments on the statistical analysis.

References

- [1] S. U. S. Choi and J. Eastman. “Enhancing thermal conductivity of fluids with nanoparticles”. In: *Proceedings of the ASME International Mechanical Engineering Congress and Exposition* 66 (1995).
- [2] S. Lee et al. “Measuring Thermal Conductivity of Fluids Containing Oxide Nanoparticles”. In: *Journal of Heat Transfer* 121.2 (1999), pp. 280–289.
- [3] B. C. Pak and Y. I. Cho. “Hydrodynamic And Heat Transfer Study Of Dispersed Fluids With Submicron Metallic Oxide Particles”. In: *Experimental Heat Transfer* 11.2 (1998), pp. 151–170.
- [4] J. A. Eastman et al. “Thermal Transport In Nanofluids”. In: *Annual Review of Materials Research* 34.1 (2004), pp. 219–246.
- [5] J. Buongiorno. “Convective Transport in Nanofluids”. In: *Journal of Heat Transfer* 128.3 (2005), pp. 240–250.
- [6] P. Keblinski, R. Prasher, and J. Eapen. “Thermal conductance of nanofluids: is the controversy over?” In: *Journal of Nanoparticle Research* 10.7 (2008), pp. 1089–1097.
- [7] J. Buongiorno et al. “A benchmark study on the thermal conductivity of nanofluids”. In: *Journal of Applied Physics* 106.9 (2009), p. 94312.
- [8] K. Khanafer and K. Vafai. “A critical synthesis of thermophysical characteristics of nanofluids”. In: *International Journal of Heat and Mass Transfer* 54.19 (2011), pp. 4410–4428.
- [9] R. Gowda et al. “Effects of Particle Surface Charge, Species, Concentration, and Dispersion Method on the Thermal Conductivity of Nanofluids”. In: *Advances In Mechanical Engineering* (2010).
- [10] J. Fan and L. Wang. “Heat conduction in nanofluids: Structure–property correlation”. In: *International Journal of Heat and Mass Transfer* 54.19 (2011), pp. 4349–4359.
- [11] J.-H. Lee, S.-H. Lee, and S. Pil Jang. “Do temperature and nanoparticle size affect the thermal conductivity of alumina nanofluids?” In: *Applied Physics Letters* 104.16 (2014), p. 161908.
- [12] R. Gangadevi, B. K. Vinayagam, and S. Senthilraja. “Effects of sonication time and temperature on thermal conductivity of CuO/water and Al₂O₃/water nanofluids with and without surfactant”. In: *Materials Today: Proceedings* 5.2, Part 3 (2018), pp. 9004–9011.
- [13] V. Mikkola et al. “Influence of particle properties on convective heat transfer of nanofluids”. In: *International Journal of Thermal Sciences* 124 (2018), pp. 187–195.
- [14] M. H. Buschmann et al. “Correct interpretation of nanofluid convective heat transfer”. In: *International Journal of Thermal Sciences* 129 (2018), pp. 504–531.
- [15] J. C. Maxwell. *A Treatise on Electricity and Magnetism*. 2nd ed. Clarendon Press, 1881, p. 435.
- [16] J. Eapen et al. “The Classical Nature of Thermal Conduction in Nanofluids”. In: *Journal of Heat Transfer* 132.10 (2010), pp. 102402–102414.
- [17] J. K. Carson et al. “Thermal conductivity bounds for isotropic, porous materials”. In: *International Journal of Heat and Mass Transfer* 48.11 (2005), pp. 2150–2158.
- [18] Z. Hashin and S. Shtrikman. “A Variational Approach to the Theory of the Effective Magnetic Permeability of Multiphase Materials”. In: *Journal of Applied Physics* 33.10 (1962), pp. 3125–3131.
- [19] I. Mugica and S. Poncet. “A critical review of the most popular mathematical models for nanofluid thermal conductivity”. In: *Journal of Nanoparticle Research* 22.5 (2020), p. 113.
- [20] N. Bouguerra, S. Poncet, and S. Elkoun. “Dispersion regimes in alumina/water-based nanofluids: Simultaneous measurements of thermal conductivity and dynamic viscosity”. In: *International Communications in Heat and Mass Transfer* 92 (2018), pp. 51–55.
- [21] P. Vadasz. “Heat Conduction in Nanofluid Suspensions”. In: *Journal of Heat Transfer* 128 (2006), pp. 465–477.
- [22] S. K. Das et al. “Temperature Dependence of Thermal Conductivity Enhancement for Nanofluids”. In: *Journal of Heat Transfer* 125.4 (2003), pp. 567–574.
- [23] C. H. Chon et al. “Empirical correlation finding the role of temperature and particle size for nanofluid (Al₂O₃) thermal conductivity enhancement”. In: *Applied Physics Letters* 87.15 (2005), p. 153107.
- [24] C. H. Li and G. P. Peterson. “Experimental investigation of temperature and volume fraction variations on the effective thermal conductivity of nanoparticle suspensions (nanofluids)”. In: *Journal of Applied Physics* 99.8 (2006), p. 84314.
- [25] C. H. Li and G. P. Peterson. “The effect of particle size on the effective thermal conductivity of Al₂O₃-water nanofluids”. In: *Journal of Applied Physics* 101.4 (2007), p. 44312.
- [26] J.-C. Yang et al. “Experimental investigation on the thermal conductivity and shear viscosity of viscoelastic-fluid-based nanofluids”. In: *International Journal of Heat and Mass Transfer* 55.11 (2012), pp. 3160–3166.

- [27] X. F. Li et al. "Thermal conductivity enhancement dependent pH and chemical surfactant for Cu-H₂O nanofluids". In: *Thermochimica Acta* 469.1 (2008), pp. 98–103.
- [28] S. Kim et al. "Experimental investigation of dispersion characteristics and thermal conductivity of various surfactants on carbon based nanomaterial". In: *International Communications in Heat and Mass Transfer* 91 (2018), pp. 95–102.
- [29] A. Nasiri et al. "Effect of dispersion method on thermal conductivity and stability of nanofluid". In: *Experimental Thermal and Fluid Science* 35.4 (2011), pp. 717–723.
- [30] F. Cao et al. "Probing Nanoscale Thermal Transport in Surfactant Solutions". In: *Scientific Reports* 5.1 (2015), p. 16040.
- [31] M. P. Beck et al. "The effect of particle size on the thermal conductivity of alumina nanofluids". In: *Journal of Nanoparticle Research* 11.5 (2009), pp. 1129–1136.
- [32] J. Bowers et al. "Flow and heat transfer behaviour of nanofluids in microchannels". In: *Progress in Natural Science: Materials International* 28.2 (2018), pp. 225–234.
- [33] M. Chandrasekar and S. Suresh. "Experiments To Explore The Mechanisms Of Heat Transfer In Nanocrystalline Alumina/Water Nanofluid Under Laminar And Turbulent Flow Conditions". In: *Experimental Heat Transfer* 24.3 (2011), pp. 234–256.
- [34] T. A. El-Brolosy and O. Saber. "Non-intrusive method for thermal properties measurement of nanofluids". In: *Experimental Thermal And Fluid Science* 44 (2013), pp. 498–503.
- [35] M. Hemmat Esfe et al. "Thermal conductivity of Al₂O₃/water nanofluids". In: *Journal of Thermal Analysis and Calorimetry* 117.2 (2014), pp. 675–681.
- [36] M. M. Heyhat et al. "Experimental investigation of turbulent flow and convective heat transfer characteristics of alumina water nanofluids in fully developed flow regime". In: *International Communications in Heat And Mass Transfer* 39.8 (2012), pp. 1272–1278.
- [37] C. J. Ho and Y. J. Lin. "Turbulent forced convection effectiveness of alumina-water nanofluid in a circular tube with elevated inlet fluid temperatures: An experimental study". In: *International Communications In Heat And Mass Transfer* 57 (2014), pp. 247–253.
- [38] J. Hong and D. Kim. "Effects of aggregation on the thermal conductivity of alumina/water nanofluids". In: *Thermochimica Acta* 542.SI (2012), pp. 28–32.
- [39] F. Iacobazzi et al. "An explanation of the Al₂O₃ nanofluid thermal conductivity based on the phonon theory of liquid". In: *Energy* 116.1 (2016), pp. 786–794.
- [40] M. H. Kayhani et al. "Experimental analysis of turbulent convective heat transfer and pressure drop of Al₂O₃/water nanofluid in horizontal tube". In: *Micro & Nano Letters* 7.3 (2012), pp. 223–227.
- [41] C. K. Kim, G.-J. Lee, and C. K. Rhee. "A study on heat transfer characteristics of spherical and fibrous alumina nanofluids". In: *Thermochimica Acta* 542.SI (2012), pp. 33–36.
- [42] N. Kumar, S. S. Sonawane, and S. H. Sonawane. "Experimental study of thermal conductivity, heat transfer and friction factor of Al₂O₃ based nanofluid". In: *International Communications in Heat and Mass Transfer* 90 (2018), pp. 1–10.
- [43] S. M. S. Murshed, K. C. Leong, and C. Yang. "Investigations of thermal conductivity and viscosity of nanofluids". In: *International Journal of Thermal Sciences* 47.5 (2008), pp. 560–568.
- [44] V. Nair, A. D. Parekh, and P. R. Tailor. "Water-based Al₂O₃, CuO and TiO₂ nanofluids as secondary fluids for refrigeration systems: a thermal conductivity study". In: *Journal of the Brazilian Society of Mechanical Sciences and Engineering* 40.5 (2018), p. 262.
- [45] D.-W. Oh et al. "Thermal conductivity measurement and sedimentation detection of aluminum oxide nanofluids by using the 3ω method". In: *International Journal of Heat and Fluid Flow* 29.5 (2008), pp. 1456–1461.
- [46] B. Ruan and A. M. Jacobi. "Investigation on Intertube Falling-Film Heat Transfer and Mode Transitions of Aqueous-Alumina Nanofluids". In: *Journal Of Heat Transfer-Transactions of the ASME* 133.5 (2011).
- [47] V. Y. Rudyak, A. V. Minakov, and S. L. Krasnolutskii. "Physics and mechanics of heat exchange processes in nanofluid flows". In: *Physical Mesomechanics* 19.3 (2016), pp. 298–306.
- [48] Z. Said et al. "Rheological behaviour and the hysteresis phenomenon of Al₂O₃ nanofluids". In: *Material Research Innovations* 18.S6 (2014), pp. 47–50.
- [49] T.-P. Teng et al. "The effect of alumina/water nanofluid particle size on thermal conductivity". In: *Applied Thermal Engineering* 30.14 (2010), pp. 2213–2218.
- [50] A. Topuz et al. "Experimental investigation of optimum thermal performance and pressure drop of water-based Al₂O₃, TiO₂ and ZnO nanofluids flowing inside a circular microchannel". In: *Journal of Thermal Analysis and Calorimetry* 131.3 (2018), pp. 2843–2863.

- [51] D. Zhu et al. "Dispersion behavior and thermal conductivity characteristics of Al₂O₃-H₂O nanofluids". In: *Current Applied Physics* 9.1 (2009), pp. 131–139.
- [52] H. A. Mints et al. "New temperature dependent thermal conductivity data for water-based nanofluids". In: *International Journal of Thermal Sciences* 48.2 (2009), pp. 363–371.
- [53] M. Modi, P. Kangude, and A. Srivastava. "Performance evaluation of alumina nanofluids and nanoparticles-deposited surface on nucleate pool boiling phenomena". In: *International Journal of Heat and Mass Transfer* 146 (2020), p. 118833.
- [54] A. Gavili and T. Isfahani. "Experimental investigation of transient heat transfer coefficient in natural convection with Al₂O₃-nanofluids". In: *Heat and Mass Transfer* (2019).
- [55] D. Khurana and S. Subudhi. "Forced convection of Al₂O₃/water nanofluids with simple and modified spiral tape inserts". In: *Heat and Mass Transfer* 55.10 (2019), pp. 2831–2843.
- [56] H. E. Patel, T. Sundararajan, and S. K. Das. "An experimental investigation into the thermal conductivity enhancement in oxide and metallic nanofluids". In: *Journal of Nanoparticle Research* 12.3 (2010), pp. 1015–1031.
- [57] A. Vakilinejad et al. "Experimental and theoretical investigation of thermal conductivity of some water-based nanofluids". In: *Chemical Engineering Communications* 205.5 (2018), pp. 610–623.
- [58] P. K. Das et al. "Stability and thermophysical measurements of TiO₂ (anatase) nanofluids with different surfactants". In: *Journal of Molecular Liquids* 254 (2018), pp. 98–107.
- [59] W. Duangthongsuk and S. Wongwises. "Measurement of temperature-dependent thermal conductivity and viscosity of TiO₂-water nanofluids". In: *Experimental Thermal and Fluid Science* 33.4 (2009), pp. 706–714.
- [60] L. R. Oliveira et al. "Thermophysical properties of TiO₂-PVA/water nanofluids". In: *International Journal of Heat and Mass Transfer* 115 (2017), pp. 795–808.
- [61] Z. Said et al. "New thermophysical properties of water based TiO₂ nanofluid—The hysteresis phenomenon revisited". In: *International Communications in Heat and Mass Transfer* 58 (2014), pp. 85–95.
- [62] S. Anbu, S. Venkatachalapathy, and S. Suresh. "Convective heat transfer studies on helically corrugated tubes with spiraled rod inserts using TiO₂/DI water nanofluids". In: *Journal of Thermal Analysis and Calorimetry* 137.3 (2019), pp. 849–864.
- [63] L. Fedele, L. Colla, and S. Bobbo. "Viscosity and thermal conductivity measurements of water-based nanofluids containing titanium oxide nanoparticles". In: *International Journal of Refrigeration* 35.5 (2012), pp. 1359–1366.
- [64] G. Singh Sokhal, D. Gangacharyulu, and V. K. Bulasara. "Influence of copper oxide nanoparticles on the thermophysical properties and performance of flat tube of vehicle cooling system". In: *Vacuum* 157 (2018), pp. 268–276.
- [65] M.-S. Liu et al. "Enhancement of thermal conductivity with Cu for nanofluids using chemical reduction method". In: *International Journal of Heat and Mass Transfer* 49.17 (2006), pp. 3028–3033.
- [66] M. Saterlie et al. "Particle size effects in the thermal conductivity enhancement of copper-based nanofluids". In: *Nanoscale Research Letters* 6.1 (2011), p. 217.
- [67] W. Guo et al. "Measurement of the thermal conductivity of SiO₂ nanofluids with an optimized transient hot wire method". In: *Thermochimica Acta* 661 (2018), pp. 84–97.
- [68] H. U. Kang, S. H. Kim, and J. M. Oh. "Estimation of Thermal Conductivity of Nanofluid Using Experimental Effective Particle Volume". In: *Experimental Heat Transfer* 19.3 (2006), pp. 181–191.
- [69] R. K. Ajeel et al. "Turbulent convective heat transfer of silica oxide nanofluid through corrugated channels: An experimental and numerical study". In: *International Journal of Heat and Mass Transfer* 145 (2019), p. 118806.
- [70] A. M. Ardekani, V. Kalantar, and M. M. Heyhat. "Experimental study on the flow and heat transfer characteristics of Ag/water and SiO₂/water nanofluids flows in helically coiled tubes". In: *Journal of Thermal Analysis and Calorimetry* 137.3 (2019), pp. 779–790.
- [71] E. Manay and E. Mandev. "Experimental investigation of mixed convection heat transfer of nanofluids in a circular microchannel with different inclination angles". In: *Journal of Thermal Analysis and Calorimetry* 135.2 (2019), pp. 887–900.
- [72] M. Rejvani et al. "Optimal characteristics and heat transfer efficiency of SiO₂/water nanofluid for application of energy devices: A comprehensive study". In: *International Journal of Energy Research* 43.14 (2019), pp. 8548–8571.
- [73] D. Singh et al. "An investigation of silicon carbide-water nanofluid for heat transfer applications". In: *Journal of Applied Physics* 105.6 (2009), p. 64306.

- [74] W. Chen et al. “Experimental investigation of SiC nanofluids for solar distillation system: Stability, optical properties and thermal conductivity with saline water-based fluid”. In: *International Journal of Heat and Mass Transfer* 107 (2017), pp. 264–270.
- [75] O. Manna, S. Singh, and G. Paul. “Enhanced thermal conductivity of nano-SiC dispersed water based nanofluid”. In: *Bulletin of Materials Science* 35 (2012).
- [76] S. Ponnada, T. Subrahmanyam, and S. V. Naidu. “An experimental investigation on heat transfer and friction factor of Silicon Carbide/water nanofluids in a circular tube”. In: *Energy Procedia* 158 (2019), pp. 5156–5161.
- [77] H. Xie et al. “Thermal Conductivity of Suspensions Containing Nanosized SiC Particles”. In: *International Journal of Thermophysics* 23.2 (2002), pp. 571–580.
- [78] N. Zouli, I. A. Said, and M. Al-Dahhan. “Enhancement of Thermal Conductivity and Local Heat Transfer Coefficients Using Fe₂O₃/Water Nanofluid for Improved Thermal Desalination Processes”. In: *Journal of Nanofluids* 8.5 (2019), pp. 1103–1122.
- [79] R. Agarwal et al. “Comparison of Experimental Measurements of Thermal Conductivity of Fe₂O₃ Nanofluids Against Standard Theoretical Models and Artificial Neural Network Approach”. In: *Journal of Materials Engineering and Performance* 28.8 (2019), pp. 4602–4609.
- [80] M. Abareshi et al. “Fabrication, characterization and measurement of thermal conductivity of Fe₃O₄ nanofluids”. In: *Journal of Magnetism and Magnetic Materials* 322.24 (2010), pp. 3895–3901.
- [81] S. Ebrahimi and S. F. Saghravani. “Experimental study of the thermal conductivity features of the water based Fe₃O₄/CuO nanofluid”. In: *Heat and Mass Transfer* 54.4 (2018), pp. 999–1008.
- [82] L. Syam Sundar, M. K. Singh, and A. C. M. Sousa. “Investigation of thermal conductivity and viscosity of Fe₃O₄ nanofluid for heat transfer applications”. In: *International Communications in Heat and Mass Transfer* 44 (2013), pp. 7–14.
- [83] Y. Gao et al. “Measurement and modeling of thermal conductivity of graphene nanoplatelet water and ethylene glycol base nanofluids”. In: *International Journal of Heat and Mass Transfer* 123 (2018), pp. 97–109.
- [84] N. Akram et al. “An experimental investigation on the performance of a flat-plate solar collector using eco-friendly treated graphene nanoplatelets–water nanofluids”. In: *Journal of Thermal Analysis and Calorimetry* 138.1 (2019), pp. 609–621.
- [85] Z. Hajjar, A. morad Rashidi, and A. Ghosatloo. “Enhanced thermal conductivities of graphene oxide nanofluids”. In: *International Communications in Heat and Mass Transfer* 57 (2014), pp. 128–131.
- [86] L. S. Sundar et al. “Thermal conductivity and viscosity of water based nanodiamond (ND) nanofluids: An experimental study”. In: *International Communications in Heat and Mass Transfer* 76 (2016), pp. 245–255.
- [87] M. Yeganeh et al. “Volume fraction and temperature variations of the effective thermal conductivity of nanodiamond fluids in deionized water”. In: *International Journal of Heat and Mass Transfer* 53.15 (2010), pp. 3186–3192.
- [88] S. H. Pourhoseini, N. Naghizadeh, and H. Hoseinzadeh. “Effect of silver-water nanofluid on heat transfer performance of a plate heat exchanger: An experimental and theoretical study”. In: *Powder Technology* 332 (2018), pp. 279–286.
- [89] Y. Bakhshan et al. “Experimental Study on the Thermal Conductivity of Silver Nanoparticles Synthesized Using Sargassum Angostifolium”. In: *Iranian Journal of Science and Technology, Transactions of Mechanical Engineering* 43.1 (2019), pp. 251–257.
- [90] Q. Li, Y. Xuan, and J. Wang. “Experimental investigations on transport properties of magnetic fluids”. In: *Experimental Thermal and Fluid Science* 30.2 (2005), pp. 109–116.
- [91] H. Jin Kim, I. C. Bang, and J. Onoe. “Characteristic stability of bare Au-water nanofluids fabricated by pulsed laser ablation in liquids”. In: *Optics and Lasers in Engineering* 47 (2009), pp. 532–538.
- [92] G. Paul, T. Pal, and I. Manna. “Thermo-physical property measurement of nano-gold dispersed water based nanofluids prepared by chemical precipitation technique”. In: *Journal of Colloid and Interface Science* 349.1 (2010), pp. 434–437.
- [93] J. Park et al. “Synthese monodisperser sphärischer Nanokristalle”. In: *Angewandte Chemie* 119.25 (2007), pp. 4714–4745.
- [94] B. L. Cushing, V. L. Kolesnichenko, and C. J. O’Connor. “Recent Advances in the Liquid-Phase Syntheses of Inorganic Nanoparticles”. In: *Chemical Reviews* 104.9 (2004), pp. 3893–3946.
- [95] R. D. Chirico et al. “Improvement of Quality in Publication of Experimental Thermophysical Property Data: Challenges, Assessment Tools, Global Implementation, and Online Support”. In: *Journal of Chemical & Engineering Data* 58.10 (2013), pp. 2699–2716.
- [96] C. A. Nieto de Castro et al. “Understanding Stability, Measurements, and Mechanisms of Thermal Conductivity of Nanofluids”. In: *Journal of Nanofluids* 6.5 (2017), pp. 804–811.

- [97] C. A. Nieto de Castro and M. J. V. Lourenço. “Towards the Correct Measurement of Thermal Conductivity of Ionic Melts and Nanofluids”. In: *Energies* 13.1 (2020).
- [98] S. Bobbo et al. “Analysis of the Parameters Required to Properly Define Nanofluids for Heat Transfer Applications”. In: *Fluids* 6.2 (2021).
- [99] A. Brunelli et al. “Agglomeration and sedimentation of titanium dioxide nanoparticles (n-TiO₂) in synthetic and real waters”. In: *Journal of Nanoparticle Research* 15.6 (2013), p. 1684.
- [100] B. P. Singh et al. “Dispersion of nano-silicon carbide (SiC) powder in aqueous suspensions”. In: *Journal of Nanoparticle Research* 9.5 (2007), pp. 797–806.
- [101] Z. Mingzheng et al. “Analysis of factors influencing thermal conductivity and viscosity in different kinds of surfactant solutions”. In: *Experimental Thermal and Fluid Science* 36 (2012), pp. 22–29.
- [102] N. Ali, J. A. Teixeira, and A. Addali. “A Review on Nanofluids: Fabrication, Stability, and Thermophysical Properties”. In: *Journal of Nanomaterials* (2018).
- [103] N. Sezer, M. Atieh, and M. Koç. “A comprehensive review on synthesis, stability, thermophysical properties, and characterization of nanofluids”. In: *Powder Technology* 344 (2018).
- [104] R. Prasher et al. “Effect of aggregation on thermal conduction in colloidal nanofluids”. In: *Applied Physics Letters* 89.14 (2006), p. 143119.
- [105] F. Jabbari, A. Rajabpour, and S. Saedodin. “Thermal conductivity and viscosity of nanofluids: A review of recent molecular dynamics studies”. In: *Chemical Engineering Science* 174 (2017), pp. 67–81.
- [106] H. Tahmooressi et al. “Numerical simulation of aggregation effect on nanofluids thermal conductivity using the lattice Boltzmann method”. In: *International Communications in Heat and Mass Transfer* 110 (2020), p. 104408.
- [107] C. Gerardi et al. “Nuclear magnetic resonance-based study of ordered layering on the surface of alumina nanoparticles in water”. In: *Applied Physics Letters* 95.25 (2009), p. 253104.
- [108] S. L. J. Thomä et al. “Atomic insight into hydration shells around faceted nanoparticles”. In: *Nature Communications* 10.1 (2019), p. 995.
- [109] M. B. Gawande et al. “Cu and Cu-Based Nanoparticles: Synthesis and Applications in Catalysis”. In: *Chemical Reviews* 116.6 (2016), pp. 3722–3811.
- [110] S. Raudenbush and S. W. Raudenbush. *HLM 6 : hierarchical linear and nonlinear modeling*. 4th print. Lincolnwood, Ill.: Scientific Software International, 2007.
- [111] A. Gelman and J. Hill. *Data analysis using regression and multilevel/hierarchical models*. Repr. with corr., 3. print. Analytical methods for social research. Cambridge: University Press, 2007.

Supplementary Material

J. Tielke, M. Maas, M. Castillo, K. Rezwan, M. Avila

1 Descriptive statistics

The following table 1a-d show descriptive statistics of the data with respect to thermal conductivity $k_{\text{eff}}/k_{\text{f}}$, the concentration φ , the temperature T , and the nanoparticle size d . Figures 1–2 show their corresponding histograms.

Table 1: Mean, minimum, maximum values and percentiles of the parameters $k_{\text{eff}}/k_{\text{f}}$, φ , T , d for all data points and the single materials.

a) Thermal Conductivity $k_{\text{eff}}/k_{\text{f}}$

		all data	Al_2O_3	TiO_2	CuO	Cu	SiO_2	SiC
mean value		1.084	1.078	1.070	1.081	1.111	1.024	1.086
minimum		0.592	0.968	0.941	1.000	1.005	0.990	1.010
maximum		1.483	1.325	1.332	1.350	1.483	1.061	1.290
percentiles	01	0.970	0.982	0.972	1.000	1.005	0.990	1.010
	05	0.990	1.002	1.006	1.0015	1.008	1.002	1.011
	10	1.000	1.015	1.014	1.017	1.021	1.007	1.017
	25	1.024	1.030	1.025	1.033	1.056	1.016	1.040
	50	1.060	1.063	1.045	1.056	1.106	1.025	1.075
	75	1.120	1.104	1.098	1.096	1.149	1.032	1.111
	90	1.220	1.172	1.154	1.201	1.205	1.040	1.208
	95	1.280	1.236	1.230	1.247	1.255	1.045	1.227
	99	1.373	1.299	1.331	1.349			

b) Concentration φ ($\cdot 10^{-2}$)

		all data	Al_2O_3	TiO_2	CuO	Cu	SiO_2	SiC
mean value		1.047	1.874	1.016	1.946	0.635	0.923	1.191
minimum		0.001	0.003	0.001	0.015	0.001	0.09	0.01
maximum		18.0	18.0	11.2	14.0	3.0	4.0	7.5
percentiles	01	0.002	0.003	0.001	0.05	0.001	0.09	0.01
	05	0.008	0.01	0.002	0.05	0.001	0.11	0.04
	10	0.02	0.025	0.003	0.1	0.023	0.13	0.04
	25	0.044	0.10	0.01	0.2	0.045	0.25	0.10
	50	0.22	1.0	0.2	0.5	0.165	0.75	0.80
	75	1.0	2.0	1.0	3.0	1.0	1.31	1.75
	90	3.0	4.0	2.54	6.0	1.30	2.0	4.0
	95	4.0	6.5	5.54	7.7	2.25	2.0	4.06
	99	11.2	15.3	11.2	13.9			

c) Temperature T

		all data	Al_2O_3	TiO_2	CuO	Cu	SiO_2	SiC
mean value		307.1	305.8	312.3	313.0	302.0	307.2	299.6
minimum		277	283	288	293	293	290	277
maximum		358	353	353	353	329	333	343
percentiles	01	283	283	288	293	293	290	277
	05	288	293	293	294	293	293	277
	10	293	293	293	298	298	293	277
	25	298	298	298	302	298	298	283
	50	303	300	313	309	298	305.5	293
	75	313.3	313	323	323	302.3	318	313
	90	328	324	333	336	316.5	323	323
	95	333	333	342.2	349	323	323	343
	99	348	344	353	353			

d) Nanoparticle size d

		all data	Al_2O_3	TiO_2	CuO	Cu	SiO_2	SiC
mean value		81.3	61.1	99.4	29.7	47.8	23.0	95.7
minimum		0.34	5	11	20	25	12	26
maximum		600	282	265	40	160	58	600
percentiles	01	0.34	05	11	20	25	12	26
	05	03	05	11	20	25	12	26
	10	10	11	11	20	25	15	26.4
	25	15	30	11	28.6	25	17	30
	50	30	45	73	29	50	25	30
	75	73	71	226	31	57.5	25	130
	90	265	150	265	40	80	25	130
	95	550	207	265	40	80	25	600
	99	550	245	265	40			

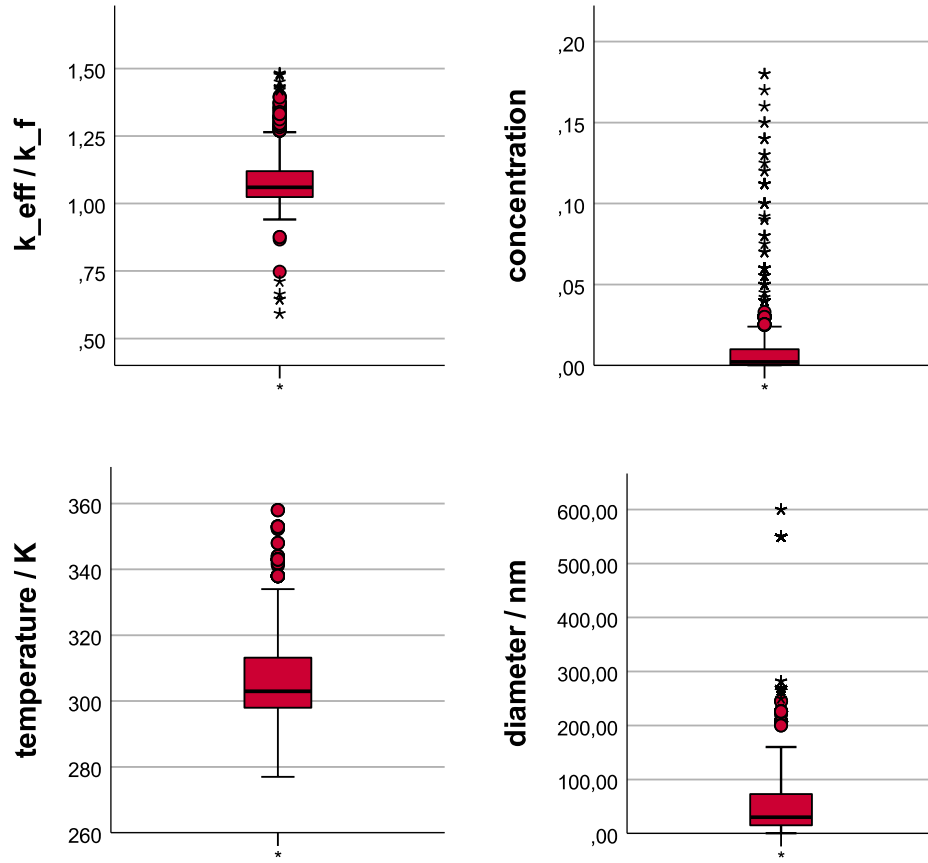


Figure 1: Boxplott diagrams showing the distribution of the data for all data points with respect to the thermal conductivity k_{eff}/k_f , concentration φ , the temperature T , and the nanoparticle size d .

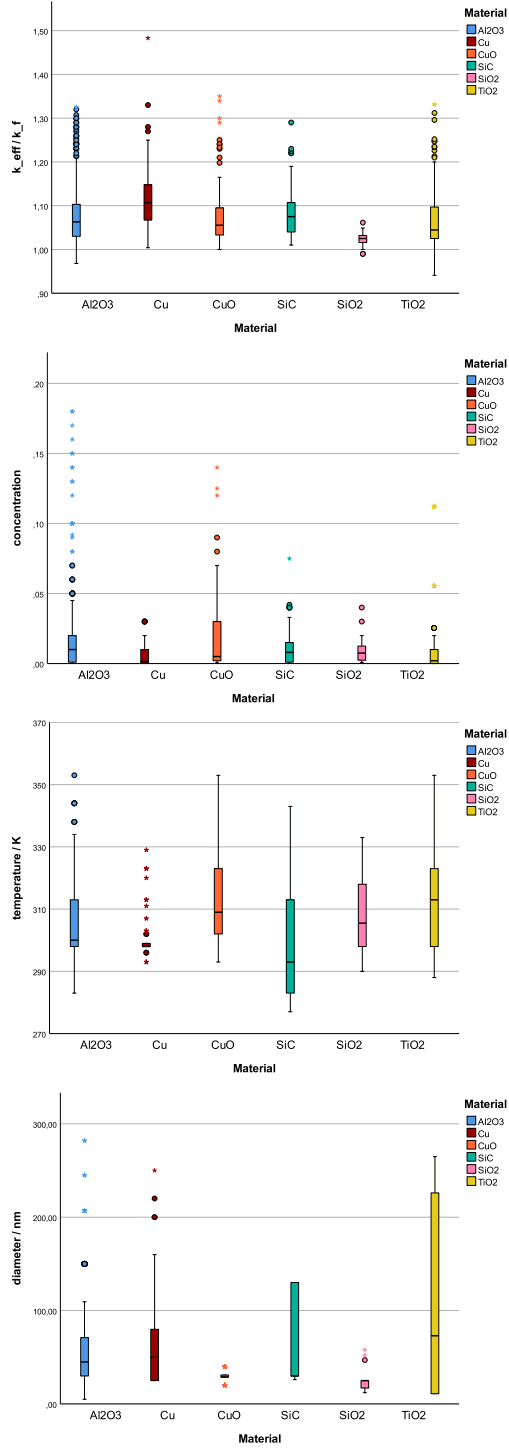


Figure 2: Boxplott diagrams showing the distribution of the data for the analyzed materials with respect to the thermal conductivity k_{eff}/k_f , concentration φ , the temperature T , and the nanoparticle size d .

2 Linear Regression

The following table 2 a-g show the results for the statistical analysis done with SPSS. Next to the general dataset, statistics were done on six single materials.

Table 2: Results for linear regression as described in section 2.1. The table shows R , R^2 , sum of squares, the coefficients with corresponding errors, 95% interval and β -values.

a) General model

R	R^2	corrected R^2	standard error	sum of squares
0.538	0.289	0.288	0.078	4.095

95% Interval					
	coefficient	error	β	lower bound	upper bound
C_0	1.031	0.003		1.025	1.037
C_φ	1.812	0.097	0.391	1.622	2.002
C_T	0.506	0.040	0.267	0.429	0.584
C_S	0.092	0.006	0.342	0.081	0.103

b) Alumina Al_2O_3

R	R^2	corrected R^2	standard error	sum of squares	
0.727	0.529	0.526	0.046	1.114	
95% Interval					
	coefficient	error	β	lower bound	upper bound
C_0	1.025	0.004		1.017	1.032
C_φ	1.748	0.079	0.715	1.594	1.903
C_T	0.311	0.048	0.209	0.216	0.406
C_S	0.164	0.043	0.123	0.080	0.248

c) Titania TiO_2

R	R^2	corrected R^2	standard error	sum of squares	
0.870	0.756	0.752	0.034	0.644	
95% Interval					
	coefficient	error	β	lower bound	upper bound
C_0	1.018	0.005		1.007	1.028
C_φ	1.694	0.111	0.579	1.476	1.913
C_T	0.629	0.046	0.512	0.538	0.721
C_S	-0.186	0.073	-0.097	-0.331	-0.041

d) Copper oxide CuO

R	R^2	corrected R^2	standard error	sum of squares
0.499	0.249	0.227	0.064	0.141

95% Interval					
	coefficient	error	β	lower bound	upper bound
C_0	1.051	0.027		0.997	1.105
C_φ	1.452	0.251	0.544	0.954	1.949
C_T	0.271	0.134	0.199	0.005	0.537
C_S	-0.473	0.754	-0.057	-1.968	1.023

e) Copper Cu

R	R^2	corrected R^2	standard error	sum of squares
0.668	0.446	0.427	0.059	0.25

95% Interval					
	coefficient	error	β	lower bound	upper bound
C_0	1.059	0.029		1.002	1.116
C_φ	7.458	1.098	0.724	5.277	9.638
C_T	-0.24	0.237	-0.086	-0.712	0.231
C_S	0.476	0.739	0.073	-0.992	1.944

f) Silica SiO_2

R	R^2	corrected R^2	standard error	sum of squares
0.541	0.292	0.266	0.011	0.004

95% Interval					
	coefficient	error	β	lower bound	upper bound
C_0	0.994	0.005		0.983	1.005
C_φ	0.608	0.170	0.351	0.269	0.947
C_T	0.104	0.032	0.311	0.040	0.168
C_S	0.415	0.085	0.469	0.245	0.585

g) Silicon carbide SiC

R	R^2	corrected R^2	standard error	sum of squares
0.837	0.700	0.682	0.036	0.150

95% Interval					
	coefficient	error	β	lower bound	upper bound
C_0	1.082	0.014		1.053	1.111
C_φ	2.965	0.366	0.702	2.229	3.701
C_T	-0.018	0.081	-0.017	-0.180	0.145
C_S	-1.246	0.440	-0.247	-2.131	-0.362

2.1 Restriction to $\varphi \leq 0.02$

As the linear regression only works for small concentrations, the data have been restricted to concentrations $\varphi \leq 0.02$. The changes in the C_φ parameter in comparison to no restriction is displayed in fig. 3 with red diamonds.

Major changes only occurred for alumina Al_2O_3 , titania TiO_2 and copper oxide CuO with an increased C_φ , which is now fitting or exceeding Maxwell's prediction. The change in the case of SiC is not in the uncertainties of the non-restricted regression, but still fits Maxwell's prediction. The changes in respect to the other materials, SiO_2 and CNT lie within their corresponding uncertainties. Higher concentrations decrease the (relative) performance of Al_2O_3 , TiO_2 and CuO , possibly due to unfavourable agglomeration effects.

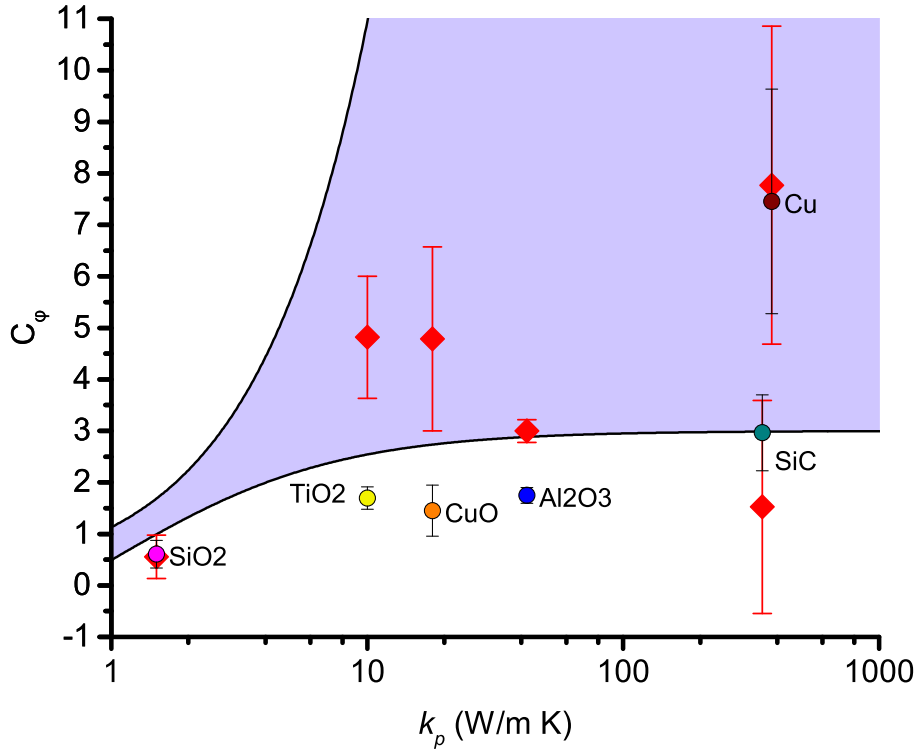


Figure 3: Thermal conductivity k_p of each material versus model parameter C_φ with corresponding 95% confidence-interval (error-bars) for linear regression. Red diamonds (including 95% error-bars) display the change in parameter C_φ with concentration $\varphi \leq 0.02$. The linearized HS-bounds are displayed as solid black line. The lower bound is given by the linearized Maxwell equation (4), whereas the upper HS-bound was calculated by linearizing the right-hand-side of eq. (2).

2.2 Use of surfactants

As the use of surfactants changes the resulting thermal conductivity, we filtered the data in which surfactants were explicitly used. This corresponds to 37%

(618 data points) of the data, which were excluded. An analysis of the different materials with the linear regression was only possible for Al_2O_3 , TiO_2 , and CuO . In the case of SiO_2 and SiC no surfactants were used and in the case of Cu only 10 data points were without the use of a surfactant, so that no linear regression is applicable. The changes in the descriptive statistics is shown in table 3 a-c. The results in the linear regression are shown in table 4 a-c and figure 4.

Table 3: Mean, minimum and maximum values of the parameters φ , T , d for the single materials Al_2O_3 , TiO_2 , and CuO with exclusion of surfactants and in comparison to with surfactant as taken from table 1.

a) Concentration φ ($\cdot 10^{-2}$)

	Without Surfactants			With Surfactants		
	Al_2O_3	TiO_2	CuO	Al_2O_3	TiO_2	CuO
mean value	2.136	1.912	2.180	1.874	1.016	1.946
minimum	0.003	0.002	0.05	0.003	0.001	0.015
maximum	18.0	11.2	14.0	18.0	11.2	14.0

b) Temperature T

	Without Surfactants			With Surfactants		
	Al_2O_3	TiO_2	CuO	Al_2O_3	TiO_2	CuO
mean value	306.2	314.7	312.4	305.8	312.3	313.0
minimum	283	288	293	283	288	293
maximum	353	353	353	353	353	353

c) Nanoparticle size d

	Without Surfactants			With Surfactants		
	Al_2O_3	TiO_2	CuO	Al_2O_3	TiO_2	CuO
mean value	47.9	58.4	28.3	61.1	99.4	29.7
minimum	5	21	20	5	11	20
maximum	282	100	40	282	265	40

Table 4: Results for linear regression as described in section 2.1 of the paper with the exclusion of surfactants. The table shows R , R^2 , sum of squares, the number of data points N , the coefficients with corresponding errors, 95% interval and β -values for Al_2O_3 , TiO_2 and CuO .

a) Alumina Al_2O_3

R	R^2	corrected R^2	standard error	sum of squares	N
0.747	0.558	0.554	0.047	1.094	405

95% Interval					
	coefficient	error	β	lower bound	upper bound
C_0	1.018	0.004		1.010	1.027
C_φ	1.788	0.082	0.735	1.626	1.950
C_T	0.340	0.052	0.224	0.238	0.442
C_S	0.245	0.047	0.174	0.152	0.338

b) Titania TiO_2

R	R^2	corrected R^2	standard error	sum of squares	N
0.945	0.893	0.889	0.030	0.576	83

95% Interval					
	coefficient	error	β	lower bound	upper bound
C_0	0.936	0.009		0.919	0.954
C_φ	1.985	0.105	0.725	1.775	2.194
C_T	0.826	0.051	0.626	0.724	0.928
C_S	1.931	0.211	0.367	1.511	2.351

c) Copper oxide CuO

R	R^2	corrected R^2	standard error	sum of squares	N
0.485	0.235	0.210	0.068	0.126	94

95% Interval					
	coefficient	error	β	lower bound	upper bound
C_0	1.063	0.034		0.996	1.131
C_φ	1.396	0.272	0.517	0.855	1.937
C_T	0.266	0.150	0.192	-0.033	0.565
C_S	-0.725	0.924	-0.080	-2.560	1.110

As to be seen in the tables, the changes due to the use of surfactants in the case of Al_2O_3 and CuO lie within their uncertainties of the regressions without restrictions. In the case of TiO_2 , the C_φ increases and is nearly in agreement with Maxwell's boundaries. The C_t also increases beyond the uncertainties of the regression without restrictions. Different to the other materials, the C_0 coefficient significantly decreases below the ideal $C_0 = 1$. Additionally, the C_S coefficient becomes significant showing a strong size-dependency.

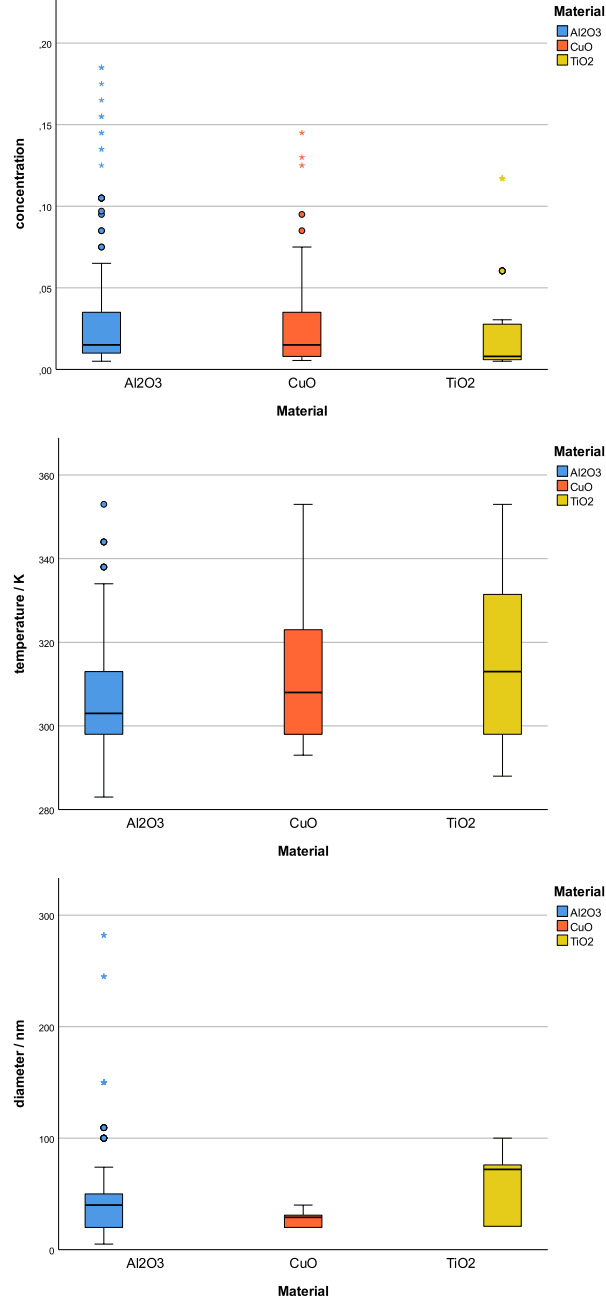


Figure 4: Histograms showing the distribution of the data with exclusion of surfactants for Al_2O_3 , CuO , and TiO_2 with respect to the concentration φ , the temperature T , and the nanoparticle size d .

2.3 Restrictions on Copper data set

The regression with all data in the case of copper resulted in a high C_0 coefficient. Out of all data sets, only the study from Liu [62] used no surfactants. Exclusion of this data set results in a significantly increased regression, which was used in the paper. The regression with all data points is again displayed in the table 5.

Table 5: Results for linear regression as described in section 2.1 with all data points (a) and without the study of Liu (b), see also table 2. The table shows R , R^2 , sum of squares, the number of data points N , the coefficients with corresponding errors, 95% interval and β -values.

a) All data points (with Liu)

R	R^2	corrected R^2	standard error	sum of squares	N
0.624	0.389	0.371	0.061	0.234	102

95% Interval					
	coefficient	error	β	lower bound	upper bound
C_0	1.098	0.021		1.056	1.140
C_φ	6.303	0.973	0.602	4.373	8.233
C_T	-0.385	0.235	-0.135	-0.851	0.082
C_S	-0.432	0.579	-0.071	-1.582	0.718

b) Without Liu

R	R^2	corrected R^2	standard error	sum of squares
0.668	0.446	0.427	0.059	0.25

95% Interval					
	coefficient	error	β	lower bound	upper bound
C_0	1.059	0.029		1.002	1.116
C_φ	7.458	1.098	0.724	5.277	9.638
C_T	-0.24	0.237	-0.086	-0.712	0.231
C_S	0.476	0.739	0.073	-0.992	1.944

The corrected correlation coefficient increases from $R^2 = 0.371$ to $R^2 = 0.427$ with the exclusion of Liu. Additionally, the C_0 coefficient decreased, while the C_φ coefficient increased.

3 Nonlinear regression

The following table 6 a-g show the results for the statistical analysis done with SPSS. Next to the general dataset, statistics were done on six single materials. The nonlinear regression is described as:

$$k^*(\varphi, S, T) = 1 + C_\varphi \varphi + C_T \Delta T + C_S \Delta S \quad (1)$$

The starting values for the coefficients were for all data and the single materials: $C_\varphi = 2$, $C_T = 0.5$, $C_S = 0.1$.

The figures 5, 6, and 7 show the coefficients as a function of the thermal conductivity of the particle material, similar to the figures with the linear regression.

Table 6: Results for nonlinear regression as described above. The table shows R^2 , the coefficients with corresponding errors and 95% interval.

a) General model

$$R^2 = 0.243$$

95% Interval				
	coefficient	error	lower bound	upper bound
C_φ	2.208	0.092	2.028	2.387
C_T	0.778	0.030	0.718	0.837
C_S	0.107	0.006	0.097	0.118

b) Alumina Al_2O_3

$$R^2 = 0.486$$

95% Interval				
	coefficient	error	lower bound	upper bound
C_φ	1.988	0.072	1.845	2.130
C_T	0.485	0.042	0.403	0.568
C_S	0.276	0.041	0.196	0.356

c) Titania TiO_2

$$R^2 = 0.741$$

95% Interval				
	coefficient	error	lower bound	upper bound
C_φ	1.791	0.110	1.574	2.008
C_T	0.731	0.036	0.660	0.802
C_S	-0.020	0.056	-0.130	0.090

d) Copper oxide CuO

$$R^2 = 0.223$$

95% Interval				
	coefficient	error	lower bound	upper bound
C_φ	1.575	0.245	1.089	2.060
C_T	0.298	0.135	0.030	0.566
C_S	0.766	0.369	0.034	1.497

e) Copper Cu

$$R = 0.244$$

95% Interval				
	coefficient	error	lower bound	upper bound
C_φ	9.089	0.776	7.547	10.630
C_T	0.017	0.206	-0.392	0.425
C_S	1.906	0.263	1.384	2.428

f) Silica SiO_2

$$R^2 = 0.281$$

95% Interval				
	coefficient	error	lower bound	upper bound
C_φ	0.500	0.142	0.218	0.783
C_T	0.087	0.029	0.030	0.144
C_S	0.331	0.043	0.246	0.415

g) Silicon carbide SiC

$$R^2 = 0.618$$

95% Interval				
	coefficient	error	lower bound	upper bound
C_φ	4.276	0.360	3.552	4.999
C_T	0.109	0.099	-0.089	0.308
C_S	0.959	0.257	0.442	1.477

3.1 Variation in concentration term

To proof that the use of the linear regression in terms of concentration is valid, we analyzed the data set with quadratic and cubic terms for the concentration parameter as shown in regressions (2) and (3). Results are shown in table 7 a-b.

$$k^*(\varphi, S, T) = 1 + C_\varphi \varphi + C_{\varphi,2} \varphi^2 + C_T \Delta T + C_S \Delta S \quad (2)$$

$$k^*(\varphi, S, T) = 1 + C_\varphi \varphi + C_{\varphi,2} \varphi^2 + C_{\varphi,3} \varphi^3 + C_T \Delta T + C_S \Delta S \quad (3)$$

The starting values for the coefficients C_φ, C_T, C_S were the same as in regression (1), while the starting values of the coefficients $C_{\varphi,2}, C_{\varphi,3}$ were set to: $C_{\varphi,2} = 1, C_{\varphi,3} = 1$.

Table 7: Results for nonlinear regression as described in regressions (2) and (3). The table shows R^2 , the coefficients with corresponding errors, and 95% interval

a) Quadratic model

$$R^2 = 0.264$$

95% Interval				
	coefficient	error	lower bound	upper bound
C_φ	3.660	0.188	3.292	4.028
$C_{\varphi,2}$	-14.921	1.694	-18.243	-11.599
C_T	0.702	0.031	0.642	0.763
C_S	0.106	0.005	0.096	0.117

b) Cubic model

$$R^2 = 0.297$$

95% Interval				
	coefficient	error	lower bound	upper bound
C_φ	5.255	0.299	4.669	5.841
$C_{\varphi,2}$	-62.083	7.131	-76.069	-48.097
$C_{\varphi,3}$	247.097	36.319	175.861	318.332
C_T	0.661	0.031	0.600	0.721
C_S	0.105	0.005	0.095	0.116

With regard to the correlation coefficient changing only some percent, the use of the linear term for the concentration is appropriate.

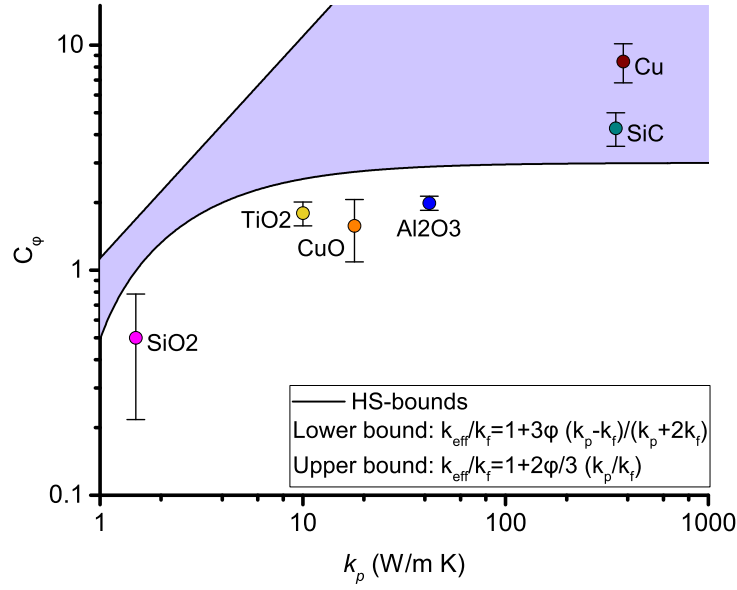


Figure 5: Thermal conductivity k_p of each material versus model parameter C_ϕ with corresponding 95% confidence-interval (error-bars) for the non-linear regression. The linearized HS-bounds are displayed as solid black line. The lower bound is given by the linearized Maxwell equation (4), whereas the upper HS-bound was calculated by linearizing the right-hand-side of eq. (2).

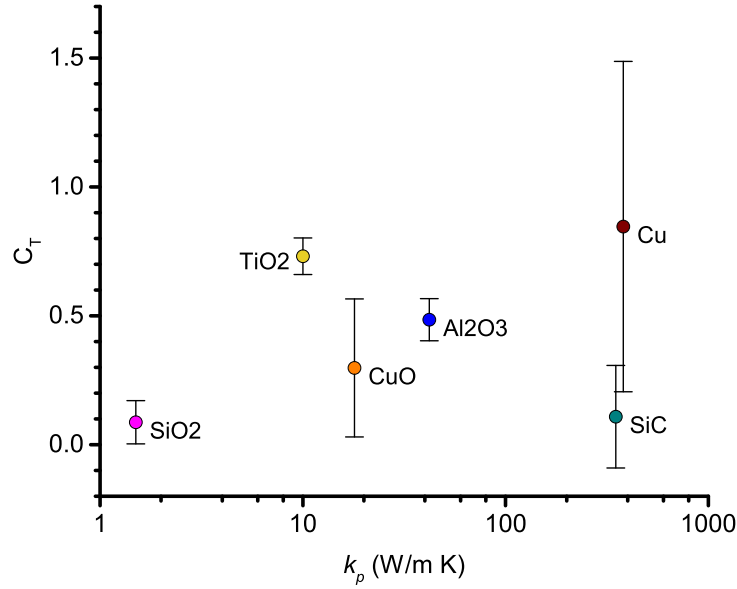


Figure 6: Thermal conductivity k_p of each material versus model parameter C_T with corresponding 95% confidence-interval (error-bars) for the non-linear regression.

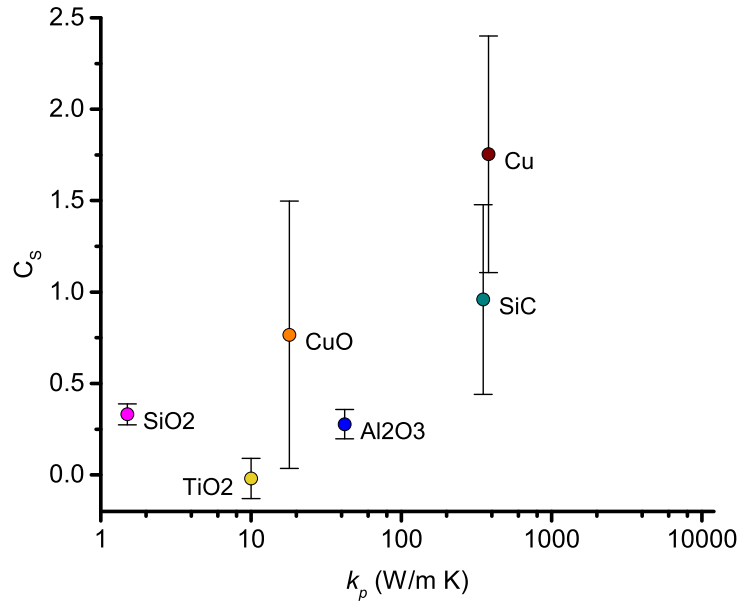


Figure 7: Thermal conductivity k_p of each material versus model parameter C_s with corresponding 95% confidence-interval (error-bars) for the non-linear regression.